

Synchrotron X-Ray Diffraction Studies on the New Generation Ferromagnetic Semiconductor Li(Zn,Mn)As under High Pressure *

Fei Sun(孙菲)^{1,2}, Cong Xu(徐丛)³, Shuang Yu(于爽)^{1,2}, Bi-Juan Chen(陈碧娟)^{1,2},
Guo-Qiang Zhao(赵国强)^{1,2}, Zheng Deng(邓正)^{1**}, Wen-Ge Yang(杨文革)^{3,4**}, Chang-Qing Jin(靳常青)^{1,2,5**}

¹Beijing National Laboratory for Condensed Matter Physics and Institute of Physics,
Chinese Academy of Sciences, Beijing 100190

²School of Physical Sciences, University of Chinese Academy of Sciences, Beijing 100049

³Center for High Pressure Science and Technology Advanced Research, Shanghai 201203

⁴High Pressure Synergetic Consortium, Geophysical Laboratory, Carnegie Institution of Washington,
Argonne 60439, USA

⁵Collaborative Innovation Center of Quantum Matter, Beijing 100871

(Received 14 March 2017)

The pressure effect on the crystalline structure of the I-II-V semiconductor Li(Zn,Mn)As ferromagnet is studied using in situ high-pressure x-ray diffraction and diamond anvil cell techniques. A phase transition starting at ~ 11.6 GPa is found. The space group of the high-pressure new phase is proposed as $Pmca$. Fitting with the Birch-Murnaghan equation of state, the bulk modulus B_0 and its pressure derivative B'_0 of the ambient pressure structure with space group of $F\bar{4}3m$ are $B_0 = 75.4$ GPa and $B'_0 = 4.3$, respectively.

PACS: 75.50.Pp, 61.05.cp, 64.60.-i

DOI: 10.1088/0256-307X/34/6/067501

Diluted magnetic semiconductors (DMS) obtained by doping transition metals (usually Mn) into semiconductors have attracted extensive studies due to their potential for manipulation of electron spin as a foundation of semiconductor spintronics.^[1–5] The proto-typical systems are the III–V based DMS, such as (Ga,Mn)As and (In,Mn)As. Substitution of divalent Mn atoms into trivalent Ga or In sites simultaneously introduces an acceptor and magnetic moments, and also leads to severely limited chemical solubility. This dual role of Mn complicates theoretical studies. Nowadays, those proto-typical ternary alloys are available only as thin films with limited Mn concentration.^[5–10] To circumvent these difficulties, Masek *et al.* first theoretically proposed the systems based on a I–II–V semiconductor LiZnAs, where the isovalent substitutional Mn impurity and carrier concentration were controlled independently by adjusting the Li-(Zn,Mn) stoichiometry.^[11] The independent spin and carrier doping is also achieved in (Ba,K)(Zn,Mn)₂As₂, which has the record reliable ferromagnetic transition temperature ($T_c = 230$ K) among DMSs.^[12,13] Thus it was regarded as a promising material for spintronics applications.^[14] Robust nearest-neighbor ferromagnetic correlations that exist above the ferromagnetic ordering temperature suggested potential to realize even higher T_c in further study.^[15] The new generation DMSs Li(Zn,Mn)As along with (Ba,K)(Zn,Mn)₂As₂ provide a unique opportunity to elucidate the intrinsic physics in DMSs and the physically transparent description of them may also be general and applicable to other DMS

materials.^[16]

LiZnAs is a direct-gap semiconductor which can be viewed as the replacement of Ga sites in (Ga,Mn)As with Li and Zn.^[17,18] It has a cubic crystal structure with space group of $F\bar{4}3m$ and its band structures obtained by local density approximation are very similar to those of GaAs.^[11] The measured band gap of LiZnAs (1.61 eV) is very close to that of GaAs (1.52 eV).^[19] Polycrystalline p-Li_{1+y}(Zn_{1-x}Mn_x)As ferromagnets with dopants up to $x = 0.15$, $y = 0.2$ were successfully synthesized by the solid state reaction method,^[20] in which magnetic moment was induced via (Zn,Mn) substitution and holes originated from excess Li. Initial values of the T_c could reach up to 50 K with ($x = 0.15$, $y = 0.1$) and small coercive field (<100 Oe) promises the application of spin manipulation.^[20] Bulk specimens of Li(Zn,Mn)As show certain advantage over proto-typical ferromagnets based on III–V semiconductors.

External pressure is an effective method to draw out the complicated interplay between structural, magnetic and electronic degrees of freedom in these novel DMSs, offering fascinating opportunities to understand the mechanism of indirect exchange interactions between dilute magnetic moments.^[21] The magnetic phase of the III–V based semiconductors, such as (Ga,Mn)As and (In,Mn)As, can be tuned by applying external pressure.^[22] In the Mn-doped II–II–V based ferromagnetic semiconductor (Ba,K)(Zn,Mn)₂As₂,^[12] by employing the combination of pressure and a suite of x-ray spectroscopy experiments (emission, absorption and dichroism), carrier-mediated ferromag-

*Supported by the National Natural Science Foundation and the Ministry of Science and Technology of China, the National Natural Science Foundation of China under Grant No U1530402, the U.S. Department of Energy of Office of Science under Grant No DE-AC02-06CH11357, the DOE-NNSA under Grant No DE-NA0001974, the DOE-BES under Grant No DE-FG02-99ER45775, and the Instrumentation Funding of National Science Foundation.

**Corresponding author. Email: dengzheng@iphy.ac.cn; yangwg@hpstar.ac.cn; jin@iphy.ac.cn

© 2017 Chinese Physical Society and IOP Publishing Ltd

netism under high pressure has been successfully studied.^[23,24] In this Letter, we focus on the structures and pressure-induced phase transition of the I-II-V based ferromagnet Li(Zn,Mn)As mainly using the in-situ high-pressure synchrotron x-ray powder diffraction (XRD).

The high-pressure powder XRD measurements were performed at room temperature at beamline 16 BM-D of the advanced photon source (APS) at Argonne national laboratory, using a Mao-Bell diamond anvil cell (DAC) with 300 μm culets. The rhenium gasket was pre-indented to 40 μm and a sample chamber 120 μm in diameter drilled in the center of the indentation. Silicone oil was used as pressure medium. Ruby balls were used to monitor the pressure. Considering that the Li(Zn,Mn)As sample is air sensitive, all the sample loading procedures were conducted in

the glove box. The x-ray wavelength was 0.31 \AA and XRD patterns were collected with an MAR 3450 image plate detector.

In-situ high-pressure synchrotron XRD measurements on $\text{Li}_{1.1}(\text{Zn}_{0.9}\text{Mn}_{0.1})\text{As}$ were performed using DAC with pressure up to 18.4 GPa. Figure 1(a) shows the XRD patterns at pressures up to 9.8 GPa. The intensity versus 2θ patterns were obtained using FIT2D software. The diffraction peaks shift to higher angles with increasing pressure, and no hint of anomalies is observed. This indicates that the structure remains the ambient pressure structure. Data analysis of the diffraction profiles was performed with the Rietveld refinements using the GSAS program package.^[25] Two typical refinement results at pressures of 1.1 GPa and 9.8 GPa are shown in Fig. 1(b), in which the fitted residuals R_{WP} are 5.6% and 2.8%, respectively.

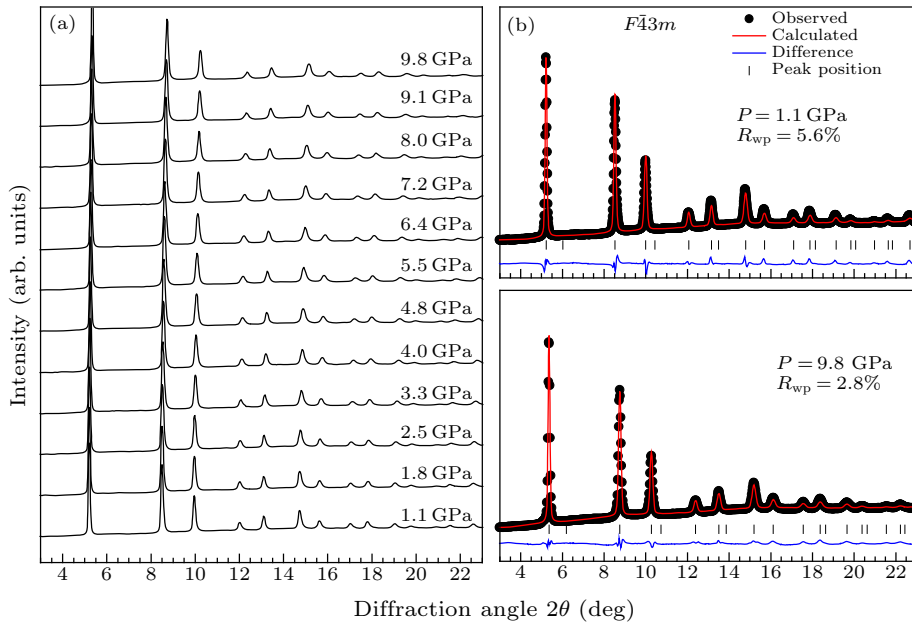


Fig. 1. (a) Synchrotron x-ray diffraction patterns of $\text{Li}_{1.1}(\text{Zn}_{0.9}\text{Mn}_{0.1})\text{As}$ at different pressures up to 9.8 GPa ($\lambda = 0.31 \text{ \AA}$), showing no hint of anomalies. (b) The observed and Rietveld refined profiles at selected pressures of 1.1 GPa and 9.8 GPa are shown with the space group of $F\bar{4}3m$. The solid circles are the experimental data, and red lines for calculated data. The positions of the Bragg reflections are marked by vertical sticks. The blue line represents the residual beneath.

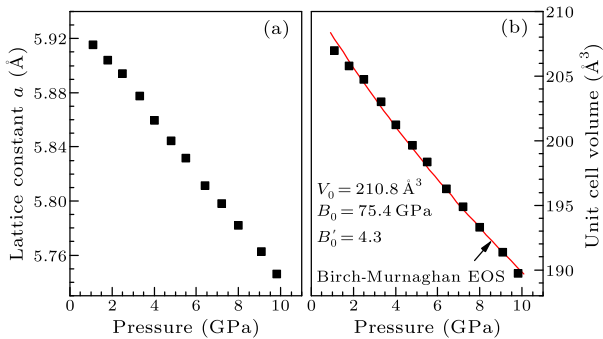


Fig. 2. (a) Pressure dependence of the lattice parameter a of $\text{Li}_{1.1}(\text{Zn}_{0.9}\text{Mn}_{0.1})\text{As}$. (b) Unit cell volume as a function of pressure. The red solid line shows the fitting data with the third-order Birch-Murnaghan equation of states and the corresponding results are also displayed.

samples are obtained from the profile refinement of the synchrotron x-ray diffraction. Figure 2(a) displays the pressure dependence of lattice parameters of $\text{Li}_{1.1}(\text{Zn}_{0.9}\text{Mn}_{0.1})\text{As}$. The lattice parameter a almost linearly decreases with increasing pressure. At the pressure of 9.8 GPa, the lattice parameter a reduces by 3.4% compared with the ambient value. Figure 2(b) presents the unit cell volume as a function of pressure (below 9.8 GPa). The volume-pressure relationship is fitted by the third-order Birch-Murnaghan equation of states,

$$P(\text{GPa}) = \frac{3}{2}B_0 \left[\left(\frac{V_0}{V} \right)^{7/3} - \left(\frac{V_0}{V} \right)^{5/3} \right] \times \left\{ 1 - \left(3 - \frac{3}{4} \times B'_0 \right) \times \left[\left(\frac{V_0}{V} \right)^{2/3} - 1 \right] \right\}. \quad (1)$$

The lattice parameters of the $\text{Li}_{1.1}(\text{Zn}_{0.9}\text{Mn}_{0.1})\text{As}$

The fitting results give the value of bulk modulus $B_0 =$

75.4 GPa with its first pressure derivative $B'_0 = 4.3$, which is very close to that of the III–V based GaAs with the experimental result $B_0 = 75.6$ GPa.^[26] This implies that Li(Zn,Mn)As is a relatively soft material.

With continuing compression beyond 9.8 GPa, a structural phase transition is clearly observed at around 11.6 GPa as shown by the appearance of new peaks. We propose the pressure-induced phase as an orthorhombic structure with space group of $Pmca$ (more will be discussed in the following). Figure 3(a) shows the XRD patterns at pressures from 9.8 GPa to 18.4 GPa. The relative intensities of the new characteristic peaks do not change much until the pressure reaches up to 14.0 GPa. Therefore, the XRD profiles in the pressure range of 11.6–14.0 GPa are attributed to a mixture of the low-pressure and high-pressure phases. With continuous compression to 18.4 GPa, the diffraction patterns remain unchanged except for a progressive right shift of all the peaks. New peaks from the high pressure phase are marked with black arrows above the profile of 14.0 GPa in Fig. 3(a). Figures 3(b) and 3(c) display the selected new peaks highlighted in shadowed areas.

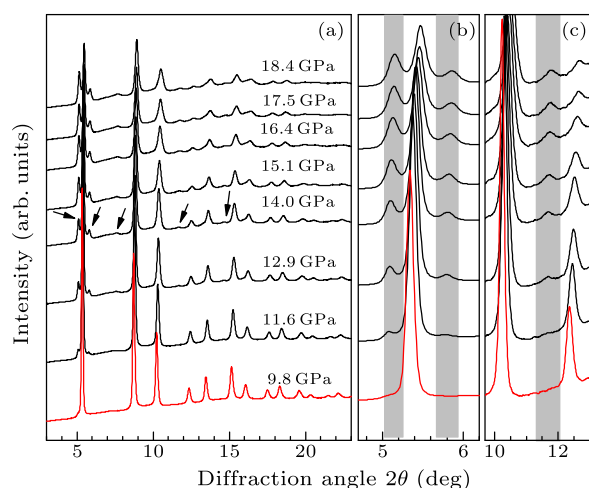


Fig. 3. (a) Synchrotron x-ray diffraction patterns of $\text{Li}_{1.1}(\text{Zn}_{0.9}\text{Mn}_{0.1})\text{As}$ at different pressures from 9.8 GPa to 18.4 GPa ($\lambda = 0.31 \text{ \AA}$). A structural phase transition starts to appear at 11.6 GPa and arrows indicate the peaks from the new structure. (b) and (c) The selected new peaks in shadowed area.

To understand the pressure-driven new phase, the software Materials Studio was employed to simulate the high pressure phase giving the optimal and physically reasonable phase structure with space group of $Pmca$. We have carried out the standard Le Bail refinement using the GSAS program and found that the high-pressure patterns indeed can be well described by the space group of $Pmca$. A typical refinement result at the pressure of 15.1 GPa is shown in Fig. 4(a), in which the fitted residual R_{WP} is 6.1%. However, the limited information obtained from powder XRD does not allow us to determine the reliable atomic position. The evolution of the lattice parameters with pressure for the high pressure new phase is displayed in Fig. 4(b). Figure 4(c) presents the unit cell volume

as a function of pressure for the low-pressure and high-pressure phases. The volume–pressure relationships fitted by the third-order Birch–Murnaghan equation of states are presented for both phases. The fitting results for the high-pressure data give the value of bulk modulus $B_0 = 84.8$ GPa with its first pressure derivative $B'_0 = 2.1$. The structural phase transition from $F\bar{4}3m$ to $Pmca$ leads to a drop of the unit cell volume of about 8% at the pressure of 11 GPa. At room temperature, similar phenomena have also been noticed in the GaAs system. When applying pressure, the structural phase transition from the zincblende structure (GaAs-I) to the orthorhombic structure GaAs-II (with proposed space group $Pmm2$) at transition pressures of 17 GPa and 11.5–13.5 GPa have been reported, respectively.^[27,28]

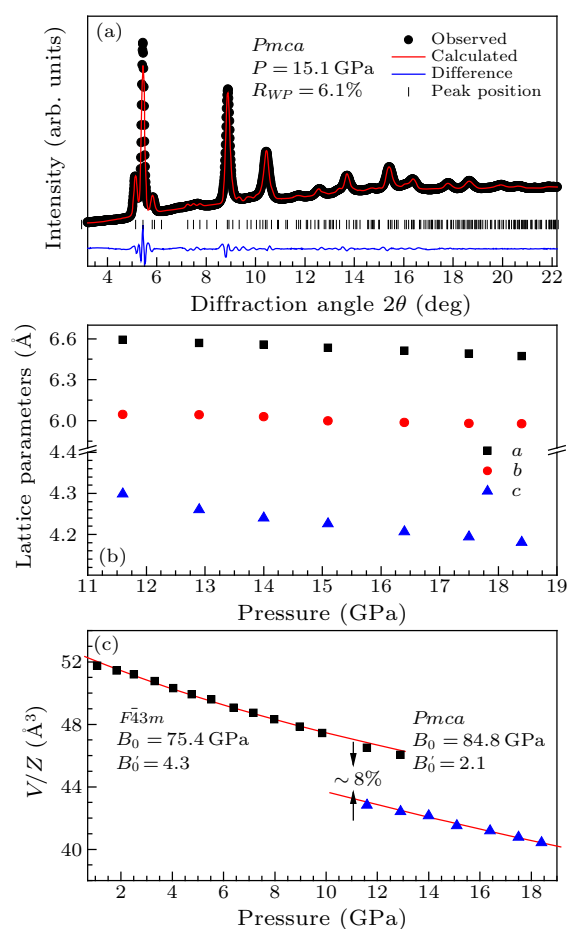


Fig. 4. (a) The observed and Le Bail refined profiles at the selected pressure of 15.1 GPa of the new phase are shown with the space group of $Pmca$. The solid circles and red lines are the experimental and calculated data, respectively. The positions of the Bragg reflections are marked by vertical sticks. The blue line represents the residual beneath. (b) Pressure dependence of the lattice parameters a , b and c for the high pressure new phase. (c) Cell volumes versus pressure. The solid lines show the fitting data with the third-order Birch–Murnaghan equation of states of ambient pressure phase ($F\bar{4}3m$) and pressure induced high-pressure phase ($Pmca$). Pressure-induced structural transition results in a collapse of the cell volume by about 8.0% at 11 GPa.

The application of pressure serves as a unique tool

for tuning the various essential parameters in semiconductors and Mn-doped DMSs.^[29,30] Pressure makes the changes in volume of solid which could modify the band structure and influences the local exchange interactions (sensitive to the interatomic distances between magnetic dopants). Therefore, high-pressure measurements are helpful in elucidating the underlying mechanisms. A number of experimental studies have been performed on the Mn-doped III–V ferromagnets: (Ga,Mn)As^[30,31] and (In,Mn)As.^[31,32] These results generally reveal that the ferromagnetic transition temperature T_c increases with pressure for samples with high concentrations of band holes. In Li(Zn,Mn)As ferromagnet, the long-range ferromagnetism between Mn dopants are mediated by carrier holes.^[11,20] Note that Li(Zn,Mn)As could be viewed as a zinc blende structure, in which Ga sites in (Ga,Mn)As are replaced with Li and Zn. Meanwhile, both ferromagnetic systems are showing comparable band structures.^[11] Considering these results, pressure could be a promising tool in enhancing the T_c in the Li(Zn,Mn)As system. Since the atomic position of the high pressure new phase has not been determined yet, the above discussion is subjected to the low pressure phase. Further studies on the exchange interactions between Mn d states under pressure would also be interesting to test theoretical band structure models.^[4]

In summary, we have presented an analysis for structures and the phase transition of ferromagnetic Li(Zn,Mn)As using in situ high-pressure x-ray powder diffraction and diamond anvil cell techniques. The lattice parameters, the bulk modulus B_0 and its pressure derivative B'_0 of ambient-pressure Li(Zn,Mn)As (space group $F\bar{4}3m$) are obtained. A pressure-driven new phase with space group of $Pmca$ is proposed. The structural phase transition leads to a contraction of the unit cell volume of about 8% after the structural phase transition. Our results on the low-pressure phase would be valuable and instructive for the future study on the ferromagnetism in Li(Zn,Mn)As.

References

- [1] Ohno H et al 1996 *Appl. Phys. Lett.* **69** 363
- [2] Ohno H 1998 *Science* **281** 951
- [3] Zutic I et al 2004 *Rev. Mod. Phys.* **76** 323
- [4] Sawicki M et al 2010 *Nat. Phys.* **6** 22
- [5] Dietl T 2010 *Nat. Mater.* **9** 965
- [6] Munekata H et al 1993 *Appl. Phys. Lett.* **63** 2929
- [7] Hayashi T et al 2001 *Appl. Phys. Lett.* **78** 1691
- [8] Hayashi T, Tanaka M, Seto K et al 1997 *Appl. Phys. Lett.* **71** 1825
- [9] Samarth N 2012 *Nat. Mater.* **11** 360
- [10] Shimizu H, Hayashi T, Nishinaga T et al 1999 *Appl. Phys. Lett.* **74** 398
- [11] Masek J, Kudrnovsky J, Maca F et al 2007 *Phys. Rev. Lett.* **98** 067202
- [12] Zhao K, Deng Z, Wang X C et al 2013 *Nat. Commun.* **4** 1442
- [13] Zhao K, Chen B, Zhao G Q et al 2014 *Chin. Sci. Bull.* **59** 2524
- [14] Hirohata A, Sukegawa H, Yanagihara H et al 2015 *IEEE Trans. Magn.* **51** 1
- [15] Frandsen B A, Gong Z, Terban M W et al 2016 *Phys. Rev. B* **94** 094102
- [16] Glasbrenner J K, Zutic I and Mazin I I 2014 *Phys. Rev. B* **90** 140403
- [17] Bacewicz R and Ciszek T F 1988 *Appl. Phys. Lett.* **52** 1150
- [18] Kuriyama K and Nakamura F 1987 *Phys. Rev. B* **36** 4439
- [19] Kuriyama K, Kato T and Kawada K 1994 *Phys. Rev. B* **49** 11452
- [20] Deng Z, Jin C Q, Liu Q Q et al 2011 *Nat. Commun.* **2** 422
- [21] Szwacki N G, Majewski J A and Dietl T 2015 *Phys. Rev. B* **91** 184409
- [22] Dietl T and Ohno H 2014 *Rev. Mod. Phys.* **86** 187
- [23] Sun F, Li N N, Chen B J et al 2016 *Phys. Rev. B* **93** 224403
- [24] Sun F, Zhao G Q, Escanhoela Jr C A et al 2017 *Phys. Rev. B* **95** 94412
- [25] Larson A C and Dreele R B V 2004 *Los Alamos Natl. Laboratory Report No. LAUR* **86** 2004
- [26] Heyd J and Scuseria G E 2004 *J. Chem. Phys.* **121** 1187
- [27] Weir S T, Vohra Y K, Vanderborgh C A et al 1989 *Phys. Rev. B* **39** 1280
- [28] Besson J M, Itie J P, Polian A et al 1991 *Phys. Rev. B* **44** 4214
- [29] Yu P Y 2011 *Phys. Status Solidi B* **248** 1077
- [30] Csontos M, Mihaly G, Janko B et al 2005 *Nat. Mater.* **4** 447
- [31] Csontos M, Mihaly G, Janko B et al 2004 *Phys. Status Solidi C* **1** 3571
- [32] Gryglas-Borysiewicz M, Kwiatkowski A, Baj M et al 2010 *Phys. Rev. B* **82** 153204